PROCEEDINGS OF SPIE

SPIEDigitalLibrary.org/conference-proceedings-of-spie

Temperature mapping using photoacoustic and thermoacoustic tomography

Haixin Ke, Todd N. Erpelding, Ladislav Jankovic, Lihong V. Wang

Haixin Ke, Todd N. Erpelding, Ladislav Jankovic, Lihong V. Wang, "Temperature mapping using photoacoustic and thermoacoustic tomography," Proc. SPIE 8223, Photons Plus Ultrasound: Imaging and Sensing 2012, 82230T (23 February 2012); doi: 10.1117/12.909000

SPIE.

Event: SPIE BiOS, 2012, San Francisco, California, United States

Temperature mapping using photoacoustic and thermoacoustic tomography

Haixin Ke[*], Todd N. Erpelding[a], Ladislav Jankovic[a], Lihong V. Wang[*]
[*]Optical Imaging Laboratory, Department of Biomedical Engineering, Washington University
1 Brookings Drive, St. Louis, MO 63130, USA;
[a]Philips Research North America, 345 Scarborough Road, Briarcliff Manor, NY 10510, USA.

ABSTRACT

Photoacoustic (PA) and thermoacoustic (TA) effects are based on the generation of acoustic waves after tissues absorb electromagnetic energy. The amplitude of the acoustic signal is related to the temperature of the absorbing target tissue. A combined photoacoustic and thermoacoustic imaging system built around a modified commercial ultrasound scanner was used to obtain an image of the target's temperature, using reconstructed photoacoustic or thermoacoustic images. To demonstrate these techniques, we used photoacoustic imaging to monitor the temperature changes of methylene blue solution buried at a depth of 1.5 cm in chicken breast tissue from 12 to 42 °C. We also used thermoacoustic imaging to monitor the temperature changes of porcine muscle embedded in 2 cm porcine fat from 14 to 28 °C. The results demonstrate that these techniques can provide noninvasive real-time temperature monitoring of embedded objects and tissue.

Keywords: Photoacoustic tomography, thermoacoustic tomography, temperature imaging.

1. INTRODUCTION

Thermotherapy is an important cancer treatment and an attractive alternative to surgery and radiation therapy [1][2][3]. The success of this application depends on how it can deposit heat to a small volume of cancerous tissue without creating an excessive temperature increase in the surrounding healthy tissue. Thus, real-time monitoring of tissue temperature is critical to avoid or minimize damage to surrounding healthy tissue.

Several methods have been used to measure temperature. Infrared thermography is a real-time method with good accuracy but it can only measure superficial temperature [4]. Ultrasound can provide measurement of good spatial resolution and penetration depth but has low temperature sensitivity [5]. Magnetic resonance imaging has the advantages of high resolution and sensitivity yet it is expensive, bulky, and slow[6][7].

Thermoacoustic tomography (TAT) provides a noninvasive means to measure temperature by monitoring temperature-induced property changes in tissue through the thermoacoustic (TA) effect. The TA effect is based on the generation of pressure waves upon absorption of electromagnetic energy[8][9]. The pressure generated is directly proportional to the local energy density absorbed in biological tissues. Absorbed energy is converted into heat, which is further converted to a pressure rise via thermoelastic expansion. This technology is also called microwave-induced thermoacoustic tomography when using microwave excitation. If the tissue is irradiated by a pulsed laser, it is referred to as photoacoustic tomography (PAT) [10][11]. TAT/PAT combines high ultrasonic resolution and high contrast due to light or radio-frequency absorption [10][11]. They can reveal dielectric or optical properties of tissues that are closely related to the physiological and pathological status of the tissues [12]. TAT/PAT have the potential to detect subtle temperature changes in tissue.

PAT has been used in calculating the temperature of fungus of the eye during laser irradiation [13]. Other studies have shown that the amplitude of photoacoustic signals from water-based and fatty tissues were directly related and proportional to the temperature [1][2][3][14]. The relationship was mostly attributed to the temperature dependent Grüneisen parameter. The temperature dependent TA signal was also studied [14].

The purpose of this paper is to establish the feasibility of using TAT/PAT to noninvasively monitor local temperature changes inside biological tissue. We monitored the TA/PA images of targets embedded in tissues during cooling or warming processes. We showed the relationship between TA/PA signals and the local temperature of the targets to

Photons Plus Ultrasound: Imaging and Sensing 2012, edited by Alexander A. Oraevsky, Lihong V. Wang,
Proc. of SPIE Vol. 8223, 82230T · © 2012 SPIE · CCC code: 1605-7422/12/$18 · doi: 10.1117/12.909000

demonstrate the possibility of monitoring relative temperature changes inside tissue. Moreover, by imaging similar targets at different positions, we demonstrated the capability of imaging relative temperature distribution.

2. METHODS AND MATERIALS

2.1 Theoretical background

The reconstructed TA or PA images are a map of the initial acoustic pressure generated by TA/PA effect. The amplitude of the acoustic pressure p can be expressed as the product of the Grüneisen parameter Γ (dimensionless), the absorption coefficient α and total deposited light or microwave energy A_e:

$$p = \Gamma \alpha A_e . \tag{1}$$

The Grüneisen parameter is a function of temperature and is determined by:

$$\Gamma = \frac{\beta v_s^2}{c_p} \tag{2}$$

where β is the thermal coefficient of volume expansion, v_s the speed of sound, and c_p the specific heat capacity, all are temperature dependent. Several previous studies have shown that that the temperature dependency of PA signal is mainly due to the Grüneisen parameter and the Grüneisen parameter of water was linearly related to the temperature [1][2][3][14]. Therefore the TA/PA pressure is correlated with the temperature as:

$$p(T) = (A + BT)\, p(T_0) \tag{3}$$

where T is the absolute temperature. T_0 is the baseline temperature which can be the room temperature. A and B are constants that depend on tissue properties. This is the basis for imaging temperature using TAT/PAT. Moreover, if we can experimentally measure the A and B for the tissue, we could measure the absolute temperature.

2.2 Imaging system description

An integrated TAT/PAT imaging system was used in this study [15][16]. The multi-modality imaging system consists of a modified clinical ultrasound system (iU22, Philips Healthcare), a microwave system, a laser system, and a data acquisition system, shown in Figure 1. The microwave system generates 3 GHz microwave pulses with different pulse widths and repetition rates and radiates pulses through a horn antenna operating at its transverse electric (TE) mode TE_{10}. The laser system has a tunable dye laser (PrecisionScan-P, Sirah), pumped by a Q-switched Nd:YAG laser (PRO-350-10, Newport). The laser beam is guided into the horn antenna through a free space optical assembly. The light is expanded by a concave lens, homogenized by a ground glass and directed onto the sample. The sample is placed on a transparent plate on top of the antenna. The microwave or laser pulses come from the bottom of the sample. An ultrasound phased array transducer (S5-1, Philips Healthcare) with 80 elements and a nominal bandwidth of 1-5 MHz is placed on top of the sample to detect the TA or PA signals. TA/PA images are reconstructed using a delay and sum beamforming algorithm.

In TAT experiments, the microwave operated at a repetition rate of 10 Hz with a pulse width of 0.3 μs. In PAT experiments, the laser had a repetition rate of 10 Hz and a pulse width of 6.5 ns. The wavelength chosen for the experiment was 650 nm. The incident laser fluence on the sample surface is controlled to be less than 20 mJ/cm^2, which is the American National Standards Institute limit[17].

The real-time temperature was measured using a precision thermistor (ON-401-PP, Omega). A voltage divider circuit converted the resistance of the thermistor into voltage, which was recorded using an oscilloscope (TDS640A, Tektronix).

2.3 Sample preparation

In the first TAT experiment, a plastic tube made of low density polyethylene (LDPE) was inserted in a piece of porcine fat/muscle tissue. Saline water was either preheated or cooled and then filled in the tube. The TA images of the saline tube were acquired while the temperature went back to room temperature by natural convection. The thermistor was immersed in the water to measure the temperature changes at the same time. In the second TAT experiment, a thin piece

of porcine muscle was either preheated or cooled and then placed between two large pieces of porcine fat/muscle tissue. The TA images of the muscle layer were obtained while the temperature changes were measured by the thermistor embedded within the muscle layer.

In the PAT experiment, two LDPE tubes filled with methylene blue (1 mM) were buried between layers of chicken breast tissue. The methylene blue solution in one tube was either preheated or cooled while that in the other tube was kept room temperature. The tubes were separated by approximately 2 cm of chicken breast tissue. Both tubes were imaged by PAT and the temperature changes of the methylene blue solution were measured by the thermistor.

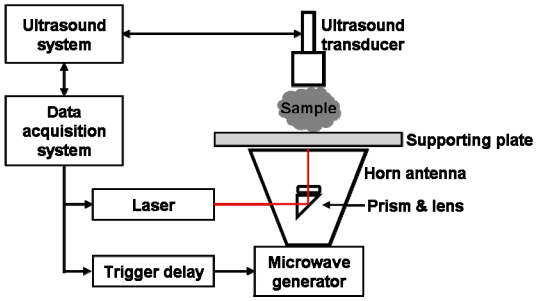

Figure 1. The main components of the system are the ultrasound system, the microwave system, the laser system, and the data acquisition system.

3. RESULTS AND DISCUSSION

The setup of the first TAT experiment was shown in Figure 2(a). The tube of saline water was inserted in a piece of porcine tissue. A thin layer of mineral oil was applied between the tube and fat to maintain acoustic coupling. The ultrasound probe was placed beside the sample to image the cross section of the tube filled with saline water. The saline water was either preheated or cooled and then filled into the tube. Both the TAT data and the temperature measurements were taken during the cooling and warming processes as the temperature of the water went to room temperature. TAT images were reconstructed after 100 averages of the raw data to improve the signal-to-noise ratio (SNR). Therefore the temporal resolution was 10 s. Improved temporal sampling can be achieved by using a more powerful microwave source or one capable of a higher repetition rate. Figure 2(b) and (c) show the TA signal amplitude calculated from TA images from 14 to 40 °C. The results show a nearly linear relationship between the TA signal and temperature. From 14 to 20 °C, the TA signal increased approximated 1.28 times, meaning a fractional change 4.5%/°C. From 22 to 40 °C, the fractional change is about 3.3%/°C. The slopes of the two curves are slightly different. This difference is most likely due to the Grüneisen parameter of water. The Grüneisen parameter increases almost linearly with temperature, but with a higher slope between 0-20 °C than between 20-100 °C [14].

Figure 3 shows the measurement results for monitoring the temperature changes from a piece of porcine muscle embedded in porcine fat. The setup is illustrated in Figure 3(a). Microwave energy was deposited into the sample from the bottom. The ultrasound transducer was placed on top of the sample. The muscle tissue was either pre-treated using hot water or cooled in a refrigerator at 4 ºC and then placed between two pieces of fat, each about 2 cm thick. The thermistor was wrapped in the muscle to measure the temperature. A TAT image of the muscle is shown in Figure 3(b). The two fat layers contained some interleaved muscle, which generated TA signals above and below the target muscle tissue. The signal from the muscle near the thermistor was chosen for analysis to avoid the signal directly from the thermistor. Therefore, a small difference exists between the real temperature and the reading from the thermistor. Figure 3(c) and Figure 3(d) show the TA signal versus temperature during the warming and cooling processes, respectively. During the warming process from 14 to 21°C the TA signal change was about 4.5%/°C and R^2 is 0.99. The TA signal change was about 6.7%/°C during the cooling process from 28 to 23 °C. The linear curve fitting gave an R^2 value of 0.98.

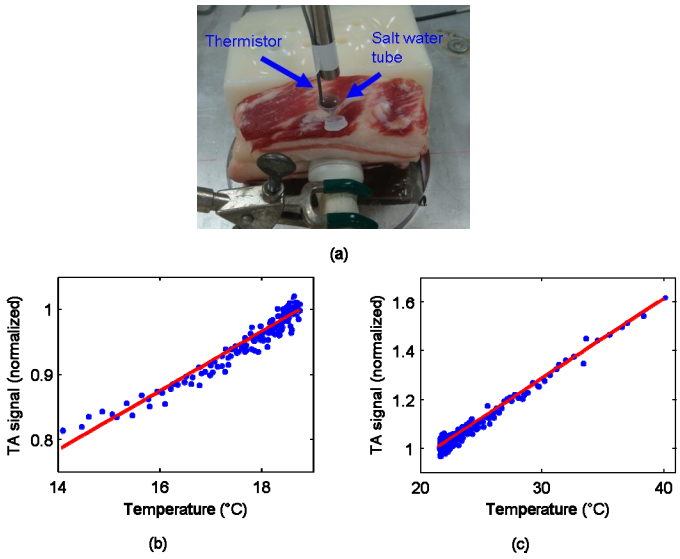

Figure 2. Imaging temperature changes of saline water in porcine tissue: a) The measurement setup. A tube of saline water was inserted in porcine tissue and was irradiated by microwave exposure from the bottom. The thermoacoustic signal was received by a transducer placed on the side of the sample. A thermistor place in the saline tube measured the temperature; b) TA signal of the embedded muscle versus temperature during warming process (dots) and the linear fitting (line); c) Normalized TA signal of the embedded muscle vs temperature during cooling process.

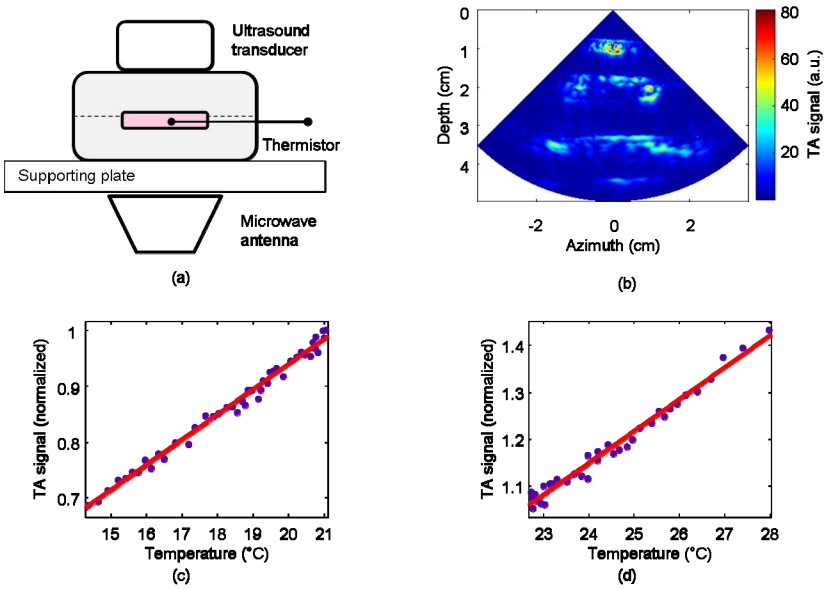

Figure 3. Imaging the temperature change of porcine muscle embedded in porcine fat: a) The measurement setup. A piece of porcine muscle placed between two pieces of fat was irradiated by microwave exposure from the bottom and the thermoacoustic signal was received by a transducer on top. A thermistor was inserted in the muscle to measure the temperature; b) A thermoacoustic image of the sample during the cooling process; c) TA signal of the embedded muscle versus temperature during warming process (dots) and the linear fitting (line). The signal was normalized by the value at 22°C predicted by the fitting; d) Normalized TA signal of the embedded muscle versus temperature during cooling process.

In the PAT experiment, two tubes filled with methylene blue solution were placed side by side between two pieces of chicken breast tissue (about 2 cm thick). Figure 4(a) illustrates the setup. The solution in the reference tube was kept at room temperature; while the in the target tube solution was preheated or cooled before filled into the tube. The two tubes were separated about 2 cm, so thermal diffusion between the tubes was negligable. The two tubes were positioned symmetrically about the center of the laser beam, so that the fluence at the two tubes was similar. A thermistor was

inserted into the target tube to measure temperature, while cross sectional PA images of both tubes were obtained simultaneously. Figure 4(b) shows a PA image of the two methylene blue tubes. PA signals were averaged 50 times to improve the SNR, yielding a temporal resolution of 5 s. The PA signal from the solution with constant temperature was proportional to the local optical power deposition and was used as a reference to eliminate the effects of laser power fluctuation. Since this reference reflects the local fluence, it is more accurate that compensation based on the surface fluence. Figure 4(c) shows the PA signal of target tube calibrated by the reference tube versus temperature measured during both cooling and warming processes. Both curves are displayed in the same plot to show the two processes match well near room temperature. The small difference of the two curves at room temperature is partly due to the temperature difference of chicken tissue surrounding the tubes. Also, the properties of the chicken tissue might change slightly because of the pre-treatment. Linear fitting of both curves gave a R^2 value of 0.99. But the slopes of the curves are different. From 11 to 19 °C, the PA signal changed 4.5%/°C; while from 21 to 44 °C, this change was 3.5%/°C.

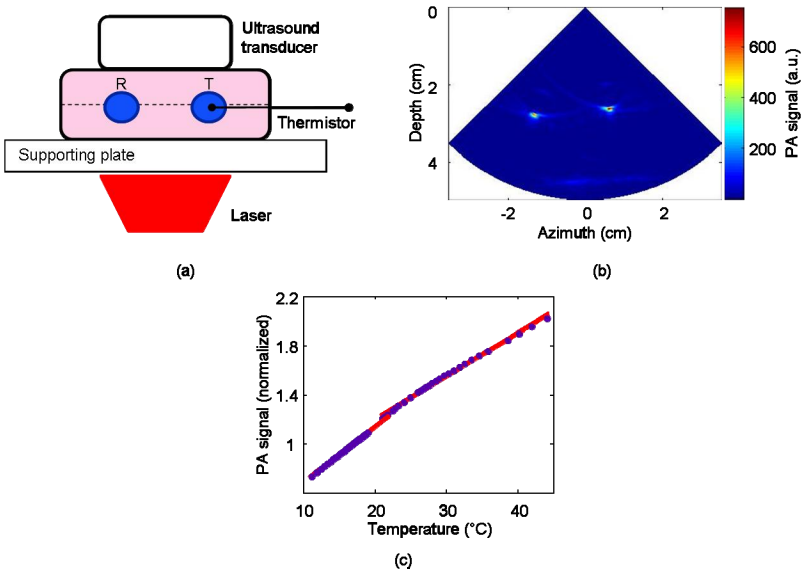

Figure 4. Imaging temperature changes of a methylene blue solution embedded in chicken breast tissue: a) The measurement setup. Two methylene blue tubes (R: reference at room temperature; T: target with changing temperature) covered by chicken breast tissue were illuminated by the laser from the bottom and the photoacoustic signal was received by a transducer on top. A thermistor was inserted in the target tube to measure the temperature; b) A photoacoustic image of the two tubes; c) PA signal of the target calibrated by that of the reference versus temperature.

In the TAT experiments, microwave energy may cause a small temperature rise (~ 1 ºC) within the samples, including the target saline water or muscle layer. While microwave heating may affect the rate of temperature change observed in TAT experiments, the relationship between the TA signals and temperature is maintained.

In the PAT experiments, two targets with different temperatures were imaged. The target with constant temperature not only provided a reference to calibrate the power fluctuations, but also demonstrates the ability to monitor relative temperature changes at different positions within the field of view (FOV). In applications such as thermal therapy using high intensity focused ultrasound, a baseline image can be taken before treatment. The PAT signal outside the heating zone can be used as a reference to compensate power fluctuations, while the PAT signal in the heating zone can monitor the temperature rise. Once tissue coagulation begins, the local absorption will change and the relationship between PAT signals and temperature will be disrupted, yet this change may still be indicative of thermal treatment. Ultrasound transducers with suitable bandwidth may be capable of measuring a continuous temperature distribution around the heating area.

Our study is not without limitations. First, the physical properties of the tissue samples are complicated and the exact relationship between tissue Grüneisen coefficients and temperature is unknown. For example, the Grüneisen coefficient of water has different temperature dependence at low and high temperatures [14]. Thus the slopes of the curves for cooling and warming processes are different. Second, the acoustic speed of sound depends on temperature but this effect was not considered since the background tissues were kept at room temperature. However, the temperature near the

target tissues was changed, so a local speed of sound change was expected. This variation introduces small errors in the results, especially in TAT experiments since the whole sample was heated by microwave.

4. CONCLUSIONS

We imaged several different targets embedded in tissue using TAT or PAT. We illustrated the linear relationship between the reconstructed TAT/PAT images and the temperature of saline water solution or muscle tissue. This suggests that both are promising techniques to monitor the temperature change of deeply embedded tissue during thermotherapy. By simultaneously imaging two targets with different temperatures using PAT, we demonstrated the possibility of creating relative temperature map of deeply embedded tissues. Although both rely on acoustic detection, TAT and PAT have different contrast mechanisms. TAT measures dominantly water/sodium contrast while PAT measures blood volume and blood oxygenation contrast. Depending on practical applications, both TAT and PAT offer non-invasive real-time temperature mapping during thermotherapy.

REFERENCES

[1] J Shah, et. al., "Photoacoustic imaging and temperature measurement for photothermal cancer therapy," Journal of Biomedical Optics 13(3), 034024 (2008).

[2] I. V. Larina, K. V. Larin, and R. O. Esenaliev, "Real-time optoacoustic monitoring of temperature in tissues," Journal of Physics D: Applied Physics, 38, 2633-2639 (2005).

[3] C. Lou, and D. Xing, "Temperature monitoring utilizing thermoacoustic signals during pulsed microwave thermotherapy: A feasibility study," International Journal of Hyperthermia, 26(4), 338-346 (2010).

[4] A. J. Welch, and M. J. C. van Gemert, Optical-thermal response of Laser-irradiated tissue. New York: Plenum (1995).

[5] R. Seip, and E. S. Ebbini, "Noninvasive estimation of tissue temperature response to heating fields using diagnostic ultrasound," IEEE Transactions on Biomedical Engineering, 42, 828-839 (1995).

[6] S. J. Graham, M. J. Bronskill, and R. M. Henkelman, "Time and temperature dependence of MR parameters during thermal coagulation of ex vivo rabbit muscle," Magnetic Resonance in Medicine, 39, 198-203 (1998).

[7] P. Steiner et. al. "Radio-frequency-induced thermoablation: Monitoring with T1-weighted and proton-frequency-shift MR imaging in an interventional 0.5-T environment," Radiology, 206, 803-810 (1998).

[8] L. V. Wang, X. Zhao, H. Sun, and G. Ku, "Microwave-induced acoustic imaging of biological tissues," Review of Scientific Instruments 70 (9), 3744-3748 (1999).

[9] R. A. Kruger, D. R. Reinecke, and G. A. Kruger, "Thermoacoustic computed tomography–technical considerations," Medical Physics 26 (9), 1832-1837 (1999).

[10] L. V. Wang, "Prospects of photoacoustic tomography," Medical Physics 35 (12), 5758-5767 (2008).

[11] M. Xu and L. V. Wang, "Photoacoustic imaging in biomedicine," Review of Scientific Instruments 77, 041101-(1-22) (2006).

[12] G. Ku, B. D. Fornage, X. Jin, M. Xu, K. K. Hunt, and L. V. Wang, "Thermoacoustic and photoacoustic tomography of thick biological tissues toward breast imaging," Technology in Cancer Research and Treatment 4 (5), 559-566 (2005).

[13] G. Schule, G. Huttmann, C. Framme, O. Roider, and R. Brinkmann, "Noninvasive optoacoustic temperature determination at the fundus of the eye during laser irradiation," Journal of Biomedical Optics, 9, 173-179 (2004).

[14] M. Pramanik, and L. V. Wang, "Thermoacoustic and photoacoustic sensing of temperature," Journal of Biomedical Optics 14(5), (2009).

[15] M. Pramanik, G. Ku, C. H. Li, and L. V. Wang, "Design and evaluation of a novel breast cancer detection system combining both thermoacoustic (TA) and photoacoustic (PA) tomography," Medical Physics 35, 2218-2223 (2008).

[16] T. N. Erpelding, C. Kim, M. Pramanik, L. Jankovic, K. Maslov, Z. Guo, J. A. Margenthaler, M. D. Pashley, and L. V. Wang, "Sentinel lymph nodes in the rat: noninvasive photoacoustic and US imaging with a clinical US system," Radiology 265 (1), 102-110 (2010).

[17] Laser Institute of America, American National Standard for Safe Use of Lasers ANSI Z136.1-2000, American National Standards Institute, Inc., New York, NY, 2000.